ION SUBSTITUTION IN THE DIOPSIDE-FERROPIGEONITE SERIES OF CLINOPYROXENES

HISASHI KUNO, *Geological Institute, Tokyo University, Tokyo, Japan.*

ABSTRACT

Evidence is presented to show that there is a complete variation in composition from augite to pigeonite passing through subcalcic augite. Under ordinary conditions of crystallization of magmas, subcalcic augite does not form; an immiscibility gap exists between augite and pigeonite. However, subcalcic augite forms only when part of Si^{4+} in Si—O chain of pyroxene is replaced by Fe^{3+}, rendering it possible for Ca^{2+}, Mg^{2+}, and Fe^{2+} to enter the pyroxene structure in all proportions. The Si^{4+}—Fe^{3+} substitution is probably favored by rapid cooling at comparatively high temperature. The course of crystallization of clinopyroxenes in the Izu-Hakone province, Japan, is from salite close to diopside, passing through augite, to ferropigeonite. Throughout the greater part of this course, Ca^{2+} of the salite is successively replaced by Fe^{2+}, while the proportion of Mg^{2+} remains nearly constant.

INTRODUCTION

This paper presents the results of the study of clinopyroxenes from volcanic rocks. The principal purpose was to solve the question whether augite and pigeonite (according to the nomenclature proposed by Poldervaart and Hess, 1951) crystallizing from magmas are continuous or is there an immiscibility gap between the two.

There is some diversity of views regarding the limit of miscibility in natural pyroxenes. Asklund (1925), Hess (1941), Edwards (1942), and Poldervaart and Hess (1951) postulate an immiscibility gap between the augite series (including ferroaugite) and the pigeonite series (including ferropigeonite, or pigeonite with Mg^{2+}: Fe^{2+} less than 1:1), although most of them consider that this gap disappears when the pyroxenes become rich in Fe^{2+} as the crystallization proceeds. This conclusion is largely based on the facts that neither clinopyroxenes having compositions intermediate between the augite and pigeonite series, namely subcalcic augite and ferroaugite, have been found in nature nor the continuous zoning between the two series has been observed. In rare cases, 2 V values change continuously from one series to the other, but Hess (Poldervaart and Hess, 1951) attributes this to an anomalous value of 2 V caused by the substitution of Al^{3+} for Si^{4+} in more than the normal amount. Edwards (a contribution to Benson's paper, 1944) regards subcalcic augite as formed metastably during rapid cooling of magmas and states that under such condition Ca^{2+} of clinopyroxenes can be replaced by Fe^{2+} without causing any undue distortion of the crystal structure.

However, the occurrence of subcalcic augite and the continuous zoning were noticed by some petrologists who concluded that a complete miscibility obtains even in less ferriferous pyroxenes (Barth, 1931*a*; Mac-

donald, 1944; Benson, 1944; Kuno, 1950). Kuno (1950) recognized the existence of the immiscibility gap between the two series with Mg^{2+}:Fe^{2+} ratio ranging from 100:0 to about 57:43.

It has been demonstrated by synthetic experiments (Bowen, 1914; Bowen, Schairer, and Posnjak, 1933) that at high temperatures clinopyroxenes form a complete solid solution except for a narrow range of composition near $FeSiO_3$. Thus, clinoenstatite-diopside solid solution is obtained at temperatures above 1300° C. and hedenbergite-ferrosilite solid solution above 950° C. While Atlas (1952) who studied subsolidus relation of the system clinoenstatite-diopside found the existence of an immiscibility gap and determined the maximum temperature of the solvus at about 1380° C.

The immiscibility gap found by Atlas extends probably towards the field of ferriferous pyroxenes, and the solvus is represented by a domed surface the crest of which would incline toward the Fe-rich side until its temperature attains a value below 950° C. at the hedenbergite-ferrosilite end of the field, as illustrated by Barth (1951).

Since the observed temperatures of basaltic lavas in active volcanoes are usually between 1200° C. and 1000° C., it is likely that the crystallization of magnesian clinopyroxenes of the basaltic magmas takes place below the temperature of the crest of the solvus surface and therefore two separate clinopyroxenes are formed.

On the other hand, the crystallization temperature of more ferriferous clinopyroxenes in strongly fractionated magmas would be above that of the crest of the solvus surface. This is indicated by the occurrence of

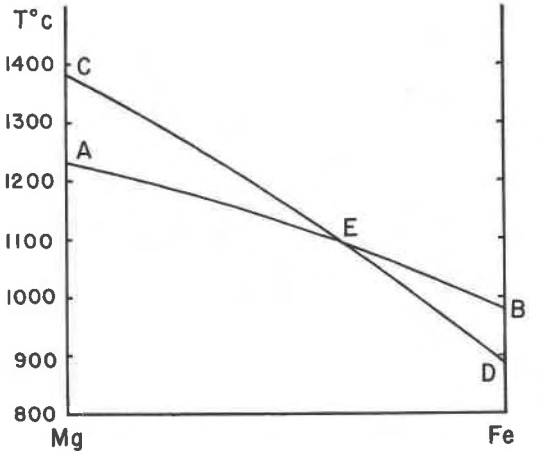

FIG. 1. Change of the crystallization temperature of magmas (*AB*) and the temperature of the crest of the solvus surface for clinopyroxenes (*CD*).

the members of the hedenbergite—ferrosilite solid solution in the Skaergaard intrusion which were first formed as members of the wollastonite solid solution and later inverted to the low temperature form (Wager and Deer, 1939, Muir, 1951).

This relation is shown diagrammatically in Fig. 1. The curve AB of the figure represents the temperatures of crystallization of the common mafic magmas at various stages of fractionation. The curve CD shows the temperature of the crest of the solvus surface.

The focus of discussion among the petrologists above cited is concerned with the location of the point E which is the intersection of the two curves.

To settle this question it is necessary to determine the range of the $Mg^{2+}:Fe^{2+}$ ratio of the pyroxenes which link the augite series with the pigeonite series, and also to examine the crystal structural relation of the two series.

Acknowledgments

This study was carried out in the Department of Geology, Princeton University, in close cooperation with Professor H. H. Hess. The writer's cordial thanks are due to the staff of the Department for many courtesies received, especially to Professor Hess for criticism of the results and for reading the manuscript. During this study, the writer was supported by the grant from The Geological Society of America (project No. 578-51) which is greatly appreciated.

Before and after his visit to Princeton, the writer engaged in the same study in the Geological Institute, Tokyo University, with the financial support by the grant from the Japanese Government Expenditure for Scientific Research.

The writer is also indebted to Dr. Kōzō Nagashima, Messrs. Takashi Katsura and Yukio Konisi for chemical analyses of pyroxenes from Hakone, Wadaki, Hatu-sima, and Ō-sima, to Assistant Professor Ryōhei Morimoto for the permission of the publication of the analyses of pyroxenes from Ō-sima made by Mr. Jōyo Ossaka, and to Dr. Akio Miyashiro for helpful discussions on the crystal chemical aspect of the problem.

X-ray Study

The chemical compositions of the pyroxenes used for the present study are listed in Tables 1–5 and are plotted in Fig. 2.

The figure shows that the diopside from St. Lawrence Co., N. Y. (Hess, 1949), and the pyroxenes Nos. 5, 6, 9, and 15 have compositions lying approximately on a straight line, and the pyroxene No. 1 close to it. This line represents the variation of the pyroxene composition largely con-

TABLE 1. COMPOSITIONS OF SALITES

	Phenocrysts		
	1	2	3
SiO_2	49.79	49.86	50.87
Al_2O_3	4.92	5.48	3.22
Fe_2O_3	0.79	2.42	0.49
FeO	5.88	4.23	7.51
MgO	14.84	15.02	14.14
CaO	22.70	22.34	23.87
Na_2O	0.20	0.00	0.32
K_2O		0.00	0.10
H_2O^+	n.d.	0.20	n.d.
H_2O^-	0.00	0.11	0.05
TiO_2	0.43	0.41	0.48
P_2O_5	tr.	0.00	n.d.
MnO	0.00	0.15	0.07
Total	99.55	100.22	101.12
Atomic no. on basis of 6 oxygen atoms			
Si^{4+}	1.851	1.837	1.883
Al^{3+}	0.149 } 2.000	0.163 } 2.000	0.117 } 2.000
Al^{3+}	0.065	0.076	0.011
Ti^{4+}	0.011	0.011	0.013
Fe^{3+}	0.022	0.066	0.013
Fe^{2+}	0.183	0.130	0.231
Mn^{2+}	0.000 } 2.024	0.004 } 2.000	0.002 } 2.026
Mg^{2+}	0.827	0.831	0.784
Ca^{2+}	0.903	0.882	0.946
Na^{1+}	0.013	0.000	0.022
K^{1+}		0.000	0.004

1. Salite in olivine eucrite (HK33010901e), an ejected block in tuff of Taga Volcano. Southwest of Wadaki near Aziro, north Izu. *Analyst*, Y. KONISI.
2. Salite in olivine-salite basalt tuff of Taga Volcano. Locality same as above. *Analyst*, S. Tanaka (Kuno and Sawatari, 1934).
3. Salite in hypersthene-salite dacite pumice (HK36082106) of Hakone Volcano. Just west of Odawara. *Analyst*, K. NAGASHIMA.

trolled by successive replacement of Ca^{2+} of the diopside by Fe^{2+} while the proportion of Mg^{2+} remains nearly constant.

These pyroxenes were selected for investigation with the North American Philips *x*-ray spectrometer. The method employed was nearly the same as that already described by Hess (1952) except that in this study the powder of pyroxene was mounted on glass slide together with

TABLE 2. COMPOSITIONS OF AUGITES

	Phenocrysts		Groundmass	
	4	5	6	7
SiO_2	51.20	51.44	50.8	50.72
Al_2O_3	2.71	2.09	2.5	0.98
Fe_2O_3	2.76	1.01	0.7	0.35
FeO	4.94	6.73	13.6	21.10
MgO	15.43	16.45	17.4	12.23
CaO	22.62	19.94	14.3	13.35
Na_2O	0.24	0.32	n.d.	0.33
K_2O	0.12	0.17	n.d.	0.13
H_2O^+	n.d.	n.d.	n.d.	n.d.
H_2O^-	0.06	0.36	n.d.	0.09
TiO_2	0.27	0.75	0.2	0.15
P_2O_5	n.d.	n.d.	n.d.	n.d.
MnO	0.05	0.21	0.4	0.37
SrO	n.d.	n.d.	n.d.	0.09
Total	100.40	99.47	99.9	99.89
Atomic no. on basis of 6 oxygen atoms				
Si^{4+}	1.885	1.911	1.906	1.960
Al^{3+}	0.115 } 2.000	0.089 } 2.000	0.094 } 2.000	0.040 } 2.000
Al^{3+}	0.000	0.005	0.019	0.006
Ti^{4+}	0.009	0.022	0.007	0.005
Fe^{3+}	0.080	0.027	0.018	0.014
Fe^{2+}	0.150	0.208	0.425	0.680
Mn^{2+}	0.002	0.007	0.014	0.012
Mg^{2+}	0.853 } 2.007	0.917 } 2.011	0.979 } 2.036	0.710 } 2.011
Ca^{2+}	0.891	0.794	0.574	0.554
Na^{1+}	0.018	0.022	0.000	0.023
K^{1+}	0.004	0.009	0.000	0.005
Sr^{2+}	0.000	0.000	0.000	0.002

4. Augite in olivine-augite basalt (HK47081901) of the Taga Volcano. Just east of Tyōzyagahara, west of Usami, north Izu. *Analyst*, K. NAGASHIMA.
5. Augite in hypersthene-olivine-augite andesite (HK35090603) of Hakone Volcano. Yagurazawa-tōge, just north of Sengokubara, northern caldera wall of Hakone. *Analyst*, K. NAGASHIMA.
6. Augite in olivine basalt (HK47040503) of Taga Volcano. Awarada-tōge, west of Usami, north Izu. *Analyst* Y. KONISI. The analysis corrected for 0.5% ilmenite impurity.
7. Augite in olivine basalt (HK47030801) of the Hatu-sima Basalt Group. Southeastern coast of Hatu-sima, north Izu. *Analyst*, K. NAGASHIMA.

TABLE 3. COMPOSITIONS OF SUBCALCIC AUGITES AND FERROAUGITE

	Groundmass		
	8	9	10
SiO_2	49.68	49.72	49.98
Al_2O_3	0.78	0.59	0.04
Fe_2O_3	3.29	3.74	1.64
FeO	18.15	18.12	23.22
MgO	16.19	16.44	12.73
CaO	9.90	9.56	11.11
Na_2O	0.65	0.42	0.29
K_2O	0.15	0.07	0.16
H_2O^+	0.10	0.17	n.d.
H_2O^-	0.00	0.00	0.12
TiO_2	0.56	0.73	0.27
P_2O_5	n.d.	n.d.	n.d.
MnO	0.59	0.78	0.27
SrO	n.d.	n.d.	0.16
Total	100.04	100.34	99.99
Atomic no. on basis of 6 oxygen			
Si^{4+}	1.896	1.903	1.958
Al^{3+}	0.037	0.028	0.000
Ti^{4+}	0.018 } 2.000	0.021 } 2.000	0.009 } 2.000
Fe^{3+}	0.049	0.048	0.033
Fe^{3+}	0.047	0.058	0.014
Fe^{2+}	0.579	0.576	0.759
Mn^{2+}	0.018	0.025	0.009
Mg^{2+}	0.927	0.943	0.747
Ca^{2+}	0.405 } 2.035	0.392 } 2.027	0.465 } 2.029
Na^{1+}	0.050	0.028	0.024
K^{1+}	0.009	0.005	0.009
Sr^{2+}	0.000	0.000	0.002

8. Subcalcic augite in hypersthene-augite basalt (HK50100803) extruded in September, 1950, from the Mihara-yama crater. Western rim of the crater, Ō-sima Island, Izu. *Analyst,* J. OSSAKA. The analysis corrected for 0.5% ilmenite impurity.
9. Subcalcic augite in hypersthene basalt (HK38031201), extruded in 1778 from the Mihara-yama crater. Western caldera floor, Ō-sima Island, Izu. *Analyst,* J. OSSAKA.
10. Subcalcic ferroaugite in coarse-grained segregation vein (HK36092301d) in hypersthene-olivine basalt lava of the Okata Basalt Group. Sea cliff at Okata, Ō-sima Island, Izu. *Analyst,* K. NAGASHIMA. The analysis corrected for 0.5% ilmenite impurity.

TABLE 4. COMPOSITIONS OF PIGEONITES

	Groundmass		
	11	12	13
SiO_2	52.84	50.56	50.28
Al_2O_3	0.44	1.41	2.03
Fe_2O_3	1.06	0.12	2.33
FeO	16.89	23.17	21.70
MgO	23.51	16.10	14.77
CaO	4.06	7.05	8.02
Na_2O	0.19	0.26	n.d.
K_2O	0.00	0.23	n.d.
H_2O^+	n.d.	n.d.	0.00
H_2O^-	0.22	0.07	
TiO_2	0.22	0.58	0.59
P_2O_5	n.d.	n.d.	0.00
MnO	0.56	0.54	0.38
SrO	0.00	n.d.	n.d.
Total	99.99	100.09	100.10
Atomic no. on basis of 6 oxygen			
Si^{4+}	1.956	1.939	1.927
Al^{3+}	0.018 } 2.000	0.061 } 2.000	0.073 } 2.000
Al^{3+}	0.000	0.003	0.019
Ti^{4+}	0.007	0.018	0.018
Fe^{3+}	0.019	0.005	0.064
Fe^{3+}	0.012	0.000	0.000
Fe^{2+}	0.522	0.741	0.692
Mn^{2+}	0.018	0.016	0.014
Mg^{2+}	1.305 } 2.030	0.927 } 2.027	0.849 } 1.985
Ca^{2+}	0.160	0.290	0.329
Na^{1+}	0.013	0.018	0.000
K^{1+}	0.000	0.009	0.000
Sr^{2+}	0.000	0.000	0.000

11. Pigeonite (microphenocrysts) in hypersthene-olivine andesite (HK47122401) of Hakone Volcano. Tengu-zawa, southeast of Hatazyuku, in the southeastern caldera wall of Hakone. *Analyst*, K. NAGASHIMA (Kuno and Nagashima, 1952).
12. Pigeonite in andesite free from pyroxene phenocrysts (HK47122301a) of Hakone Volcano. Upper course of the Sukumo-gawa valley near the confluence of Kiwada-zawa, southeastern caldera wall of Hakone. *Analyst*, K. NAGASHIMA.
13. Pigeonite (with admixture of augite) in aphyric andesite (HK33081909a) of Hakone Volcano. Saru-sawa, south of Yumoto, eastern caldera wall of Hakone. *Analyst*, I. IWASAKI (Kuno, 1940).

TABLE 5. COMPOSITION OF PIGEONITE AND FERROPIGEONITES

	Phenocrysts			
	14	15	16	17
SiO_2	50.40	49.30	49.72	48.90
Al_2O_3	1.99	0.68	0.90	3.86
Fe_2O_3	0.13	3.83	1.72	4.65
FeO	21.30	23.17	27.77	25.35
MgO	18.28	15.38	12.69	6.87
CaO	6.43	3.14	3.80	7.96
Na_2O	1.33	n.d.	0.23	0.58
K_2O	0.02	n.d.	0.12	0.20
H_2O^+	n.d.	n.d.	1.27	0.57
H_2O^-	n.d.	n.d.	0.08	0.35
TiO_2	0.55	0.60	0.85	0.12
P_2O_5	n.d.	n.d.	n.d.	n.d.
MnO	n.d.	2.44	0.98	0.51
Total	100.43	98.54	100.13	99.92
	Atomic no. on basis of 6 oxygen			
Si^{4+}	1.907	1.930	1.965	1.940
Al^{3+}	0.091 } 2.000	0.033	0.035 } 2.000	0.060 } 2.000
Al^{3+}	0.000	0.000 } 2.000	0.008	0.121
Ti^{4+}	0.002	0.019	0.026	0.005
Ti^{4+}	0.014	0.000	0.000	0.000
Fe^{3+}	0.005	0.018	0.000	0.000
Fe^{3+}	0.000	0.095	0.052	0.138
Fe^{2+}	0.672	0.760	0.915 } 1.970	0.838 } 1.924
Mn^{2+}	0.000 } 2.089	0.080	0.033	0.017
Mg^{2+}	1.037	0.909 } 1.976	0.751	0.409
Ca^{2+}	0.261	0.132	0.161	0.338
Na^{1+}	0.100	0.000	0.019	0.048
K^{1+}	0.000	0.000	0.005	0.010

14. Pigeonite (with admixture of augite) in augite-pigeonite-hypersthene andesite (HK33022001) of Hakone Volcano. North of Hakone-tōge, southern caldera wall of Hakone. *Analyst*, T. SAMESHIMA (Kuno, 1952).
15. Ferropigeonite in remelted quartz diorite (HK37090503), an ejected block in pumice of Hakone Volcano. Northeast of Yumoto, eastern flank of Hakone. *Analyst*, T. KATSURA.
16. Ferropigeonite in ferropigeonite andesite. Loch Scridain, Mull, Scotland. *Analyst*, E. G. RADLEY (Hallimond, 1914).
17. Ferropigeonite (with admixture of ferroaugite) in ferropigeonite andesite (HK40110106). North of Ōkubo-yama, Minami-Aizu, Hukusima Prefecture. *Analyst*, T. INOUE (Kuno and Inoue, 1949).

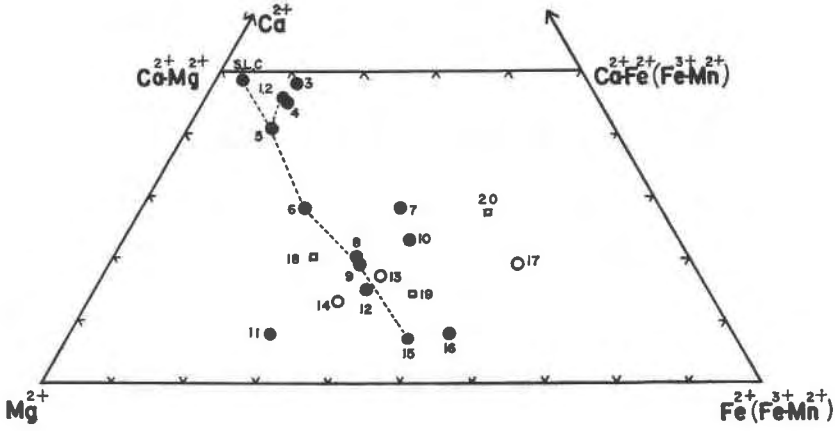

FIG. 2. Compositions of clinopyroxenes in atomic per cent. The numbers refer to those in Tables 1–5 and 10. S.L.C.—diopside from St. Lawrence Co. Solid circle—single pyroxene phase. Open circle—mixture of two clinopyroxene phases. Square—pyroxene whose composition was determined by partial analysis and by optical constants.

silicon powder used as an internal standard for calibration.

The unit cell dimensions a', b, and c', were determined from the 2θ angles for the reflections {750}, {660}, {260}, {060}, {350}, {600}, {440}, {150}, {510}, {041}, {330}, {002}, {310}, {220}, {021}, {020}, and {200}, and the angle β from 2θ for $\{53\bar{1}\}$, {531}, {331}, $\{31\bar{1}\}$, $\{22\bar{1}\}$, {131}, {311}, and {221} and the already known values of a', b, and c'. All measurements were made with Cu K_α radiation filtered by nickel. The values of a and c were then calculated from a', c', and β. The cleavage angle $110 \wedge 1\bar{1}0$ were calculated from a' and b.

A part of the results of this study has been already published (Kuno and Hess, 1953). It has been demonstrated that all the common clinopyroxenes belong to the same space group as diopside C_{2h}^6, $C\ 2/c$, and that the unit cell dimensions change continuously with the ratio $Ca^{2+}:Mg^{2+}:Fe^{2+}$ $(+Fe^{3+}+Mn^{2+})$ of the pyroxenes.

The x-ray powder diffraction patterns for these pyroxenes are shown in Fig. 3, and the unit cell dimensions a, b, and c, and the angles β and $110 \wedge 1\bar{1}0$ are listed in Table 6 and plotted in Fig. 4.

The angles β and $110 \wedge 1\bar{1}0$ show straight-line variation from the diopside to the ferropigeonite. The value of a also changes continuously throughout the series. No discontinuity is to be seen between the augite and the ferropigeonite.

A curve is drawn to show the variation of the b values of the clinopyroxenes with Al^{3+} content less than 0.05 (the diopside and the py-

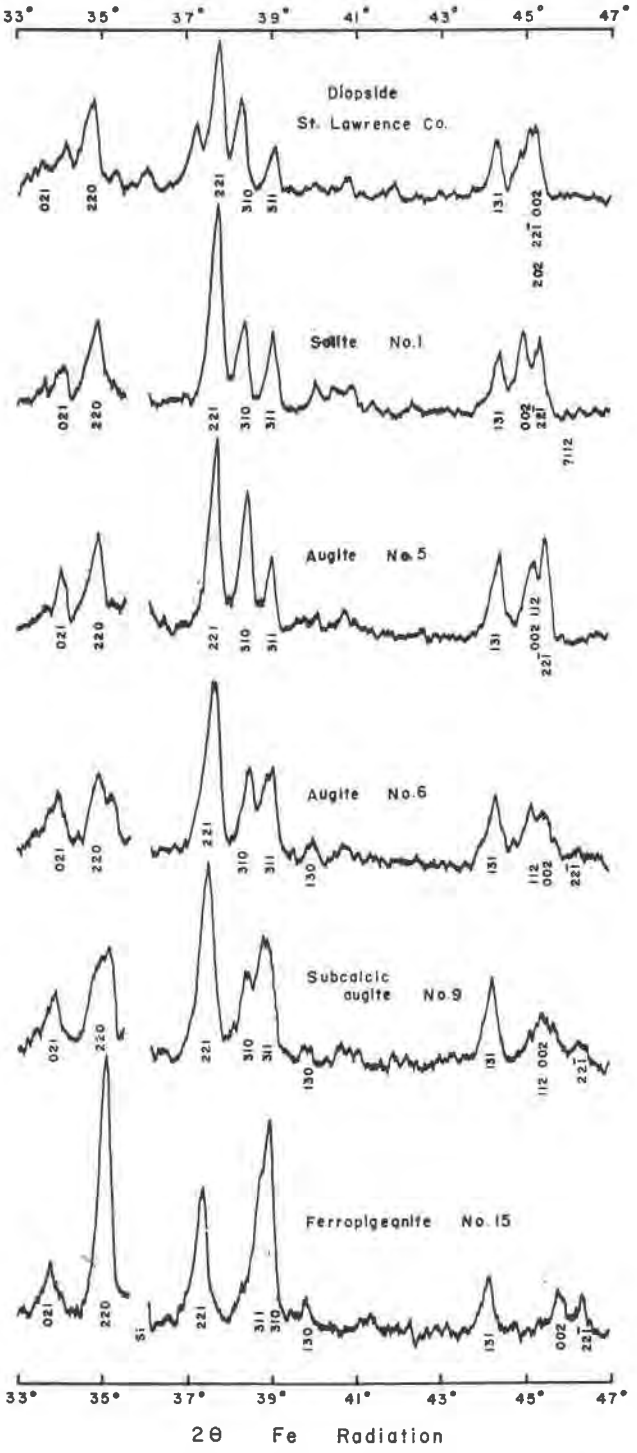

FIG. 3. *X*-ray powder diffraction patterns for the pyroxenes of the diopside-ferropigeonite series.

TABLE 6. UNIT CELL DIMENSIONS AND THE CRYSTALLOGRAPHIC ANGLES OF THE DIOPSIDE—FERROPIGEONITE SERIES

	Diopside St. Lawrence Co. $Ca_{49}Mg_{47}Fe_4$	No. 1 Salite, Wadaki $Ca_{46}Mg_{43}Fe_{11}$	No. 5 Augite, Yagurazawa-tōge $Ca_{41}Mg_{47}Fe_{12}$
a	9.750 Å	9.742 Å	9.744 Å
b	8.930	8.901	8.909
c	5.249	5.268	5.260
β	74°10′	73°55′	73°28′
$110 \wedge 1\bar{1}0$	87°12′	87°07′	87°18′
	No. 6 Augite, Awarada-tōge $Ca_{28}Mg_{49}Fe_{23}$	No. 9 Subcalcic augite Ō-sima $Ca_{19}Mg_{46}Fe_{35}$	No. 15 Ferropigeonite Yumoto $Ca_7Mg_{45}Fe_{48}$
a	9.722 Å	9.716 Å	9.712 Å
b	8.925	8.944	8.959
c	5.242	5.242	5.251
β	72°57′	72°20′	71°27′
$110 \wedge 1\bar{1}0$	87°40′	88°02′	88°26′

roxenes Nos. 9 and 15, Table 7). The b values of Nos. 1, 5, and 6 which contain higher Al^{3+} (Table 7) lie below this standard curve. Two curves are drawn tentatively, one representing the b values for pyroxenes with Al^{3+} about 0.2 and another for those with Al^{3+} about 0.1. The effect of Al^{3+} is also seen in the c value; the values for the pyroxenes Nos. 1 and 5 lie above the standard curve constructed for the c value of the pyroxenes with lower Al^{3+} content.

TABLE 7. ATOMIC NUMBERS OF Al^{3+} IN PYROXENES ON THE BASIS OF 6 OXYGENS

	St. Lawrence Co.	No. 1	No. 5	No. 6	No. 9	No. 15
Al^{3+}	0.018	0.214	0.094	0.113	0.028	0.033

The Al^{3+} content does not appear to affect the a value.

The contraction of b length of the unit cell and the expansion of c are also found in orthorhombic pyroxenes, although in the latter the expansion of c takes place only to a limited extent (Hess, 1952).

It might be suggested that the expansion of c is caused by the substitution of the Al^{3+} ions for the smaller Si^{4+} ions, while the contraction of b

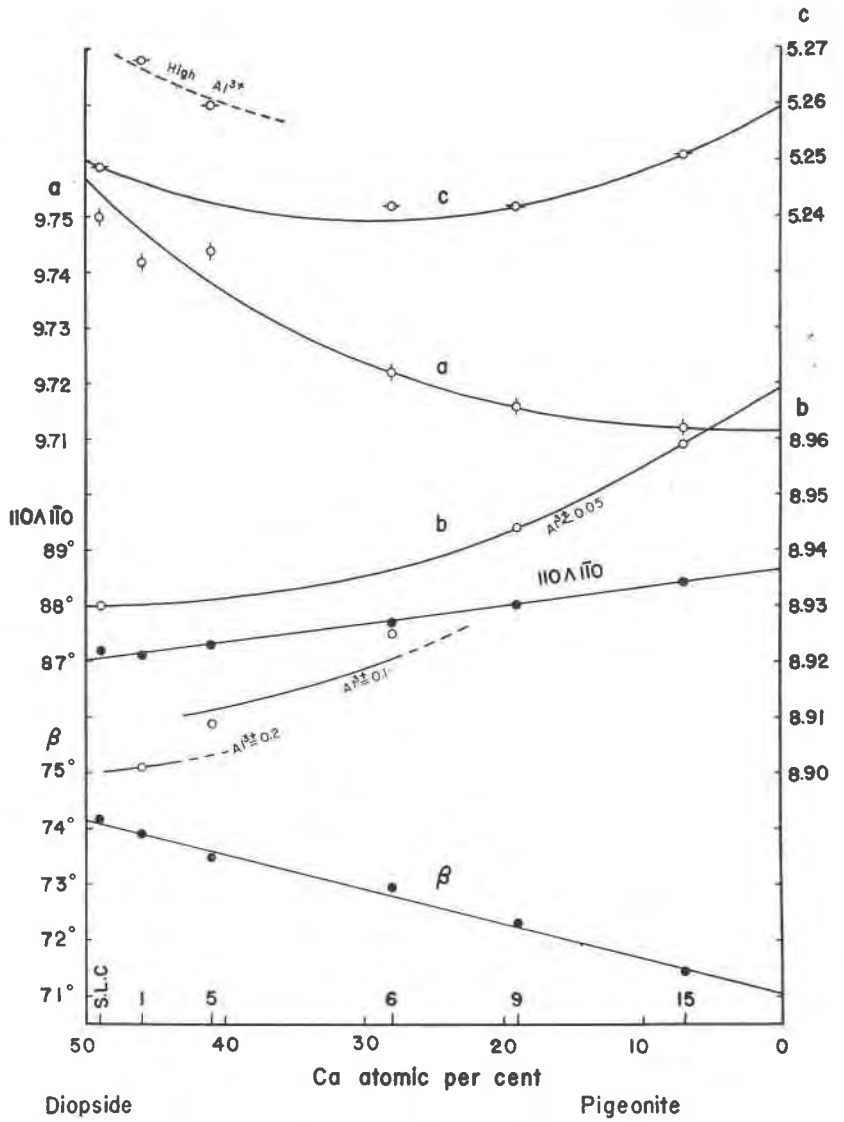

FIG. 4. Variation of the unit cell dimensions and crystallographic angles for the diopside-ferropigeonite series.

by the substitution of the Al^{3+} ion for the larger Mg^{2+} ion. Hess (1952), on the other hand, considered that, in orthopyroxenes, the substitution of Al^{3+} for Si^{4+} at first increases the c value but larger amounts of Al^{3+} causes the SiO_3 chain to zigzag in the 010 plane and hence no more increase of c. The zigzag in the 010 plane and the substitution of Al^{3+} for

Mg^{2+} result in the contraction of b without changing a. In any case, the more marked increase of c in the clinopyroxenes than in the orthopyroxenes is probably due to the higher proportion of Al^{3+} in the Si^{4+} position in the former.

The crystal structure of the clinoenstatite-pigeonite-ferrosilite series appears to be unique among clinopyroxenes belonging to C_{2h}^6. As shown in Table 8, the angle $110 \wedge 1\bar{1}0$ of this series is about 1° larger than those of any other clinopyroxenes, and the angle β from 4° to 1° lower than those of the latter except spodumene.

TABLE 8. CRYSTALLOGRAPHIC ANGLES OF CLINOPYROXENES

	Diopside (Kuno and Hess, 1953)	Hedenbergite (Kuno and Hess, 1953)	Acmite (Dana, 1900)	Spodumene (Dana, 1900)	Jadeite (Yoder, 1950)
$110 \wedge 1\bar{1}0$	87°12′	86°46′	87°04′	87°00′	87°02′
β	74°10′	75°40′	73°11′	69°40′	72°44.5′
	Clinoenstatite (Kuno and Hess, 1953)	Pigeonite No. 11 (Kuno and Hess, 1953)	Ferropigeonite No. 15	Ferropigeonite from slag (Bowen, 1933)	Ferrosilite from lithophysae (Bowen, 1935)
$110 \wedge 1\bar{1}0$	88°04′	88°17′	88°26′	88°40′	89°10′
β	71°38.5′	71°27′	71°27′	71°31′	n.d.

The angle β for ferrosilite is probably about 71° 35′ as inferred by extrapolation, and this value and the value of $110 \wedge 1\bar{1}0$ for the same pyroxene are very different from those of hedenbergite with which it forms a solid solution. This departure of the angles from those of the Ca-rich pyroxenes might explain the extreme rarity of ferrosilite.

The subcalcic augite No. 9 shows a strong zoning from pigeonite to augite, and one might doubt that the mineral consists of a mixture of two separate phases, pigeonite and augite, and that the apparently continuous zoning is due to anomalous value of 2V. In Fig. 5 the powder diffraction pattern of the pyroxene No. 9 is compared with that of a mixture of the augite No. 7 and the pigeonite No. 11 in the ratio 1:1.

The mixture shows double peaks in the pattern while No. 9 shows single broad peaks at the corresponding positions. It is safe to conclude that the subcalcic augite represents a single phase.

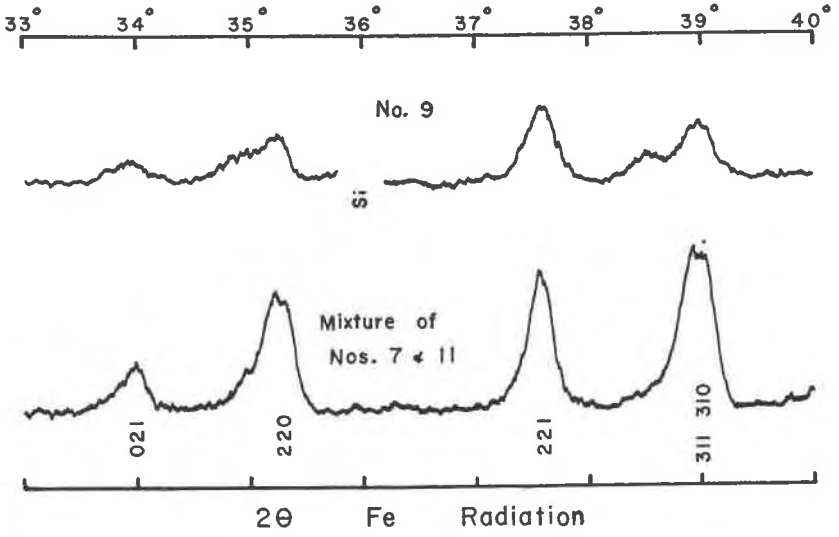

FIG. 5. *X*-ray powder diffraction patterns in the single pyroxene No. 9 and of the mixture of the two pyroxenes Nos. 7 and 11.

TABLE 9. OPTICAL CONSTANTS OF THE PYROXENES

	Diopside* St. Lawrence Co.	No. 1	No. 5	No. 6
α (mean)	1.6718	1.690	1.690	1.691
β (mean)	1.6785	1.696	1.696	1.697
γ (mean)	1.7013	1.715	1.716	1.718
Range of β	none	0.009	0.008	0.006
(+) 2V (in 010)	56°5	59°	51°	44°
Range	3°5	3°	5°	10°
Dispersion	$r>v$	$r>v$	$r>v$	no disp.
	No. 8	No. 9	No. 10	No. 15
α (mean)	1.709	1.711	1.719	1.713
β (mean)	1.711	1.713	1.722	1.713
γ (mean)	1.738	1.739	1.745	n.d.
Range of β	0.042	0.043	0.068	0.003
(+) 2V (in 010)	28°	25°	29°	11°
Range	30°	41°	47°	20°
Dispersion	$r<v$	$r<v$	no disp.	$r<v$

* Hess, 1949.

Optical Study

The mean values of refractive indices and 2V of the pyroxenes of the diopside-ferropigeonite series are given in Table 9.

The 2V value changes continuously through this series. The refractive indices of the pyroxenes Nos. 1 and 5 are much higher than those of the diopside, probably due to the high Al^{3+} content, and the range of refractive indices of the subcalcic augite No. 9 is very great.

In Table 9 are also given the optical constants of the subcalcic augites Nos. 8 and 10. The 2V values of these pyroxenes and of No. 9 vary continuously from about 10° (core) to about 40° (margin), the optic plane being always parallel to 010. The values between 20° and 35° are quite common, although these values were considered previously as extremely rare in clinopyroxenes.

Similar continuous zoning has been observed in some other crystals as shown in Table 10. Their mean compositions are plotted in Fig. 2.

Table 10. Zoning in Clinopyroxenes

	No. 18	No. 19	No. 20
β	1.685–1.731	1.704–1.710	1.710–1.733
(+) 2V	0° (core) →39° (margin) (in 010)	46° (core) →0° (margin) (in 010)	0° (core) →51° (margin) (in 010)
Composition	$Ca_{20}Mg_{53}Fe_{27}$* (mean)	$Ca_{37}Mg_{34}Fe_{29}$ (core) $Ca_{10}Mg_{42}Fe_{48}$ (margin)	$Ca_{10}Mg_{42}Fe_{48}$ (core) $Ca_{37}Mg_{13}Fe_{50}$ (margin)

* Partial analysis by Nagashima.

The subcalcic augite No. 18 occurs in the groundmass of basalt from Okata, Ō-sima Island, Izu, and shows quite similar zoning as those in Nos. 8, 9, and 10.

Porphyritic clinopyroxenes (No. 19) in andesite from Weiselberg, Germany, consist of augite and ferropigeonite (Kuno, 1947). Where the two types of pyroxenes occur in the same crystal, they are either zoned continuously as shown in Fig. 6 or bounded distinctly from one another.

Clinopyroxene crystals (No. 20) about 1 mm. in length occur in pegmatitic schlieren in a dolerite sheet at Semi, Yamagata Prefecture, Japan. Some of the crystals are zoned continuously but others show discontinuous zoning.

Crystal Chemistry

The general formula for pyroxenes may be written as follows (Berman, 1937; Hess, 1949):

$(W)_{1-p}\,(X,\,Y)_{1+p}Z_2O_6$
$W = Ca^{2+}, Sr^{2+}, Na^{1+}, K^{1+}$
$X = Mg^{2+}, Fe^{2+}, Mn^{2+}, Ni^{2+}$
$Y = Al^{3+}, Fe^{3+}, Cr^{3+}, Ti^{4+}$
$Z = Si^{4+}, Al^{3+}, Ti^{4+}, Fe^{3+}$

The atomic proportions of the pyroxenes listed in Tables 1–5 are calculated on the assumption that the number of atoms in the Z group always amounts to 2.000. If addition of Al^{3+} to Si^{4+} does not satisfy the number of atoms required for the Z group, then Ti^{4+} and Fe^{3+} are also added until the total number of these atoms becomes 2.000. Al^{3+}, Ti^{4+}

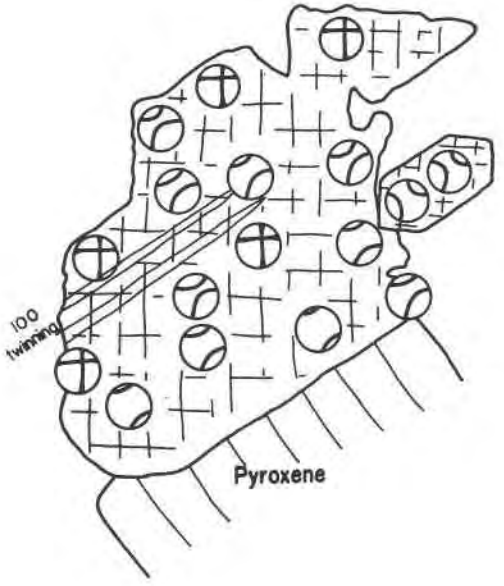

FIG. 6. Variation of the optic angle 2V in a pyroxene phenocryst (0.25 mm. long) in andesite from Weiselberg.

and Fe^{3+} left after this allotment then constitute the Y group. The total number of atoms of the W, X, and Y groups for the pyroxenes listed in the tables except Nos. 14 and 17 approximately equals 2.000, indicating that these pyroxenes have the theoretical compositions. In the case of the pyroxenes Nos. 14 and 17, the cause of the departure from the theoretical formula is not known. It is certainly not due to impurities.

In the subcalcic augites Nos. 8, 9, and 10, considerable proportion of Fe^{3+} (0.05 to 0.03) and all of Ti^{4+} enter the Z group, otherwise the compositions do not fit the theoretical formula. In all other pyroxenes except Nos. 11 and 15, Fe^{3+} does not enter this group. In Nos. 11 and 15, the amount of Fe^{3+} in the Z group is only 0.02.

That a part of Si^{4+} in the pyroxene structure can be replaced by Ti^{4+} has been discussed by Barth (1931*b*), Dixon and Kennedy (1933), and Muir (1951), but the replacement by Fe^{3+} has not been anticipated.

The entrance of Fe^{3+} in the tetrahedral position of silicate is demonstrated by the existence of Fe^{3+}-bearing potash-feldspars both as natural and synthetic minerals (Faust, 1936; Rosenqvist, 1951). A small amount of Fe^{3+} enters this position in plagioclase of Skaergaard intrusion (Wager and Mitchell, 1951) and also in anorthite from Wadaki, north Izu (Kuno, 1950).

Ahrens (1952) gave the following ionic radii of the cations for 6-fold co-ordination:

$$Si^{4+}\ 0.42, \qquad Al^{3+}\ 0.51, \qquad Fe^{3+}\ 0.64, \qquad Ti^{4+}\ 0.68.$$

The similarity of the ionic radius indicates that Fe^{3+} and Ti^{4+} are equally capable of replacing Si^{4+}, although other factors such as the ionization potential and electronic charge of the two ions may also affect the capability of substitution.

The partial substitution of Fe^{3+} for Si^{4+} appears to be characteristic of subcalcic augite and ferroaugite, or pyroxenes with compositions lying within the postulated immiscibility gap. Since the analyses listed in the tables were made by many different analysts, the relation cannot be considered to be fortuitous.

As shown in Fig. 2, the analyzed pyroxenes other than Nos. 8, 9, 10, and 18 consist either of a single phase with Ca^{2+} content more than 25 per cent or less than 15 per cent or of a mixture of the two phases.

About 10 excellent analyses of porphyritic augites from Japanese volcanic rocks could be cited. They all have Fe^{3+} in the *Y* group. Hess (1949) listed 44 first-class analyses of clinopyroxenes, and only one of them (No. 40) has Fe^{3+} in the *Z* group. This pyroxene is aegirinaugite and may be set aside from the present discussion.

Of the 23 clinopyroxenes from the Skaergaard intrusion listed by Muir (1951), only three (Nos. 11, 13, and 14) contain Fe^{3+} in the *Z* group, but the amount of Fe^{3+} in this group is less than 0.02. In another pyroxene (No. 12), the amount of Fe^{3+} in the *Z* group attains 0.038, but the revised analysis of this pyroxene by Muir revealed that all Fe^{3+} enters the *Y* group.

At temperatures of dry melts, Ca^{2+} of diopside can be replaced by Mg^{2+} and Fe^{2+}, probably in all proportions except for those corresponding to ferrosilite. However, at temperatures prevailing in ordinary magmas, this replacement can take place until the ratio $Ca^{2+}:Mg^{2+}+Fe^{2+}=25:75$ is attained. This limit is represented approximately by the pyroxenes Nos. 6 and 7. Further replacement causes undue distortion of the structure, and the pyroxenes just beyond this limit (subcalcic augite and ferroaugite) are no longer stable, breaking up into two phases, namely,

that with Ca^{2+} more than 25 per cent and that with Ca^{2+} less than 15 per cent. The structure of the latter pyroxene is probably suitable for accommodating the smaller ions Mg^{2+} and Fe^{2+} in place of the larger ion Ca^{2+}, and therefore can form at ordinary magmatic temperature as a stable phase.

However this distortion of the structure is released by the entrance of the large Fe^{3+} ion in the tetrahedral position, and therefore subcalcic augite and ferroaugite can form.

Conditions Necessary for the Formation of Subcalcic Augite

The temperature of crystallization of the subcalcic augite No. 8 has been measured. The lava from which the mineral was separated was extruded from the Mihara-yama crater, Ō-sima Volcano, in the middle of September, 1950. At the lava fountain, the temperature was 1100° C. (Minakami, 1951 *a*), and at the rim of the crater about 500 meters away from the fountain, it was from 1070° C. to 1030° C. as measured by the writer using an optical pyrometer. At 1030° C. the lava was still fluid. Where the temperature fell below 1000° C., the lava nearly stopped moving. Examination of the specimens of the lava showed that the final movement was due to the fluidity of the glass present interstitially between pyroxene and plagioclase. The rock specimen for the pyroxene separation was collected on October 8th at the crater rim when it was still hot. It contains also a little interstitial glass. Scoriaceous fragments ejected from the lava fountain are made up largely of glassy groundmass with some scattered phenocrysts.

Thus it may be concluded that the groundmass pyroxene (No. 8) started to crystallize at some temperature a little below 1100° C. and ceased to grow at about 1000° C.

The subcalcic augite No. 9 was separated from the 1778 lava of the same crater. Judging from the similarity of the chemical composition and surface feature of this lava to those of 1951 lava, the temperatures of these lavas at the time of extrusion were nearly the same. The temperature of the 1951 lava at the lava fountain was estimated as about 1200° C. (Minakami, 1951 *b*).

The subcalcic ferroaugite No. 10 and the subcalcic augite No. 18 occur in basaltic segregation veins in the same olivine-pyroxene basalt flow.

Pyroxenes having similar compositions (2V from 30° to 20°) occur in the groundmass of basalts but are rare in that of andesites. They are extremely rare, if not entirely absent, in gabbros and dolerites, as has been pointed out by many authors.

Since the common gabbros and dolerites were formed probably at temperatures nearly the same as those observed in the Ō-sima lavas, the conclusion may be drawn that rapid cooling at comparatively high

temperatures favors the formation of subcalcic augite and ferroaugite and also pyroxenes with continuous zoning.

It may be assumed that at high temperatures the magma consists of Si^{4+}—O^{2-}, Al^{3+}—O^{2-}, Ti^{4+}—O^{2-}, and Fe^{3+}—O^{2-} tetrahedra and freely moving cations. During rapid cooling, Si^{4+}—O^{2-} tetrahedra would be linked with Fe^{3+}—O^{2-} tetrahedra to form the $(Si^{4+}, Fe^{3+})O_3^{2-}$ chain of pyroxene. This framework would be able to accommodate Ca^{2+}, Mg^{2+}, and Fe^{2+} without limitation in their proportion. On the other hand, during slow cooling, $(Si^{4+}, Fe^{3+})O_3^{2-}$ chain might be once formed but equilibrium adjustment would take place and Fe^{3+} in the chain would be successively replaced by Si^{4+} and Al^{3+}, resulting in the ordinary $(Si^{4+}, Al^{3+})O_3^{2-}$ chain. This framework would be able to take up Ca^{2+}, Mg^{2+}, and Fe^{2+} to a certain limited extent. Even during slow cooling, some crystals in a rock or some part of a crystal would have the $(Si^{4+}, Fe^{3+})O_3^{2-}$ framework which has escaped from equilibrium adjustment. This would account for the rare occurrence of continuously zoned pyroxenes as phenocrysts and as crystals in some dolerite pegmatites.

The crystal chemical aspect pictured above may be expressed in another way.

Thus, where a small proportion of Fe^{3+} enters the tetrahedral position in pyroxenes, the temperature of the solvus for such pyroxenes becomes lower than that for the normal pyroxenes. The temperatures of magmas now lie above this solvus temperature, and therefore subcalcic augite and ferroaugite can form as stable phases.

Referring to Fig. 1, the curve *CD* is displaced downward for the series of pyroxenes with some Fe^{3+} in the tetrahedral position, so that the point *E* moves toward the point *A* of the figure. The point lies at least on the Mg-rich side of the point No. 18 of Fig. 2 ($Mg^{2+}:Fe^{2+}=65:35$) for pyroxenes with about 0.040 Fe^{3+}.

On the other hand, the normal magnesian pyroxenes of the common mafic magmas crystallize below the solvus temperature, and the point *E* lies at about $Mg^{2+}:Fe^{2+}=35:65$ as determined by Wager and Deer (1939).

The position of the point *E* also moves easily according to the temperatures of the magmas. In andesitic magmas, the point *E* moves further toward the Fe-rich side, as shown by the pyroxene No. 17 which consists of two distinct clinopyroxenes with the average ratio $Mg^{2+}:Fe^{2+}=29:71$.

Poldervaart and Hess (1951) and Kuno and Nagashima (1952) used the term "two-pyroxene boundary" for the line in the ternary diagram Ca^{2+}—Mg^{2+}—Fe^{2+} which has the same significance as the point *E* of the binary diagram Fig. 1. However the term was first introduced by Tsuboi (1932) for the boundary line in the ternary diagram which sepa-

rates the field of augite from that of hypersthene. The term should be used according to the original definition by Tsuboi.

Crystallization of Pyroxenes from Japanese Magmas

The course of crystallization of clinopyroxenes in a strongly fractionated basaltic magma has been completely traced by Muir (1951). The trend of differentiation of the basaltic and andesitic magmas of Izu-Hakone province, Japan, is slightly different from that of the Skaergaard magma (Kuno, 1953). The crystallization of clinopyroxenes in the pigeonitic rock series of this province (Kuno, 1950) can be discussed on the basis of the analyses plotted in Fig. 2, although the figure also includes two pyroxenes from other localities which represent the later stage of the pyroxene crystallization in this province.

The pyroxenes Nos. 1, 2, and 4 are early-formed phenocrysts in basaltic magmas. They were separated before orthopyroxene starts to crystallize, and have compositions close to diopside; only a small proportion of Ca^{2+} of diopside is replaced by Fe^{2+}. These pyroxenes have high contents of Al^{3+} mostly in tetrahedral position.

The pyroxene No. 3 which forms phenocrysts in dacite pumice has an exceptionally high content of Ca^{2+}.

The pyroxene No. 5 forms phenocrysts in mafic hypersthene-augite andesite and represents a slightly more advanced stage of crystallization.

As the crystallization proceeds, the amount of Ca^{2+} replaced by Fe^{2+} increases continuously until the limit of miscibility, approximately represented by Nos. 6 and 7, is attained. Nos. 6 and 7 are later-formed crystals in basaltic magmas (groundmass).

Upon further crystallization, the ratio $Ca^{2+}:Mg^{2+}+Fe^{2+}$ in the pyroxene becomes lower than 25:75, and Ca^{2+} can no longer be replaced either by Fe^{2+} or Mg^{2+} except when rapid cooling at high temperatures obtains. At this stage, the composition of the magma becomes andesitic and its temperature is usually not high enough to permit this replacement even if rapid cooling obtains, so that the pyroxenes split into two phases, one with Ca^{2+} higher than 25 per cent and another lower than 15 per cent. Such a stage is represented by the pyroxenes Nos. 13, 14, and 17, including intratelluric crystals and groundmass grains.

In certain cases, rapid cooling of high-temperature magma results in the formation of the pyroxenes with Ca^{2+} content between 25 and 15 per cent. Such pyroxenes are found in the groundmass of pyroxene basalts (Nos. 8, 9, 10, and 18).

In more advanced stages of the crystallization of the andesitic magmas, Ca^{2+} of the pyroxenes is largely replaced by Fe^{2+}, resulting in pigeonites and ferropigeonites with $Ca^{2+}:Mg^{2+}+Fe^{2+}$ less than 15 per cent. The

compositions of such pyroxenes are shown by the analyses Nos. 12, 15 and 16. Optical examination of groundmass pyroxenes of salic andesites showed that they have compositions close to those of Nos. 15 and 16.

The latest stage of the pyroxene crystallization is represented by ferropigeonite occurring in cavitites of dacite (Kuno, 1950). It has a composition $Ca_8Mg_{28}Fe_{64}$.

Thus throughout the main part of the course of crystallization of pyroxenes, Ca^{2+} of the magnesian salite is successively replaced by Fe^{2+} and the content of Mg^{2+} of the pyroxenes remains nearly constant.

In the Skaergaard intrusion, the earliest pyroxene has the same composition as the salite of Japan. In the earlier stage of the pyroxene crystallization, Ca^{2+} is replaced by Fe^{2+} to a certain extent, and thereafter the main trend is controlled by the Mg^{2+}—Fe^{2+} substitution. The earlier trend is comparable to the main trend of the Japanese pyroxenes.

The pyroxene No. 11 is a member of a series which follows a different course of crystallization. In this series, orthopyroxene separates first and is followed by successively more calcic clinopyroxenes (Kuno and Nagashima, 1952). Thus Mg^{2+} of the pyroxene No. 11 is gradually replaced by Ca^{2+} and Fe^{2+} until the pyroxene has composition of subcalcic augite or Ca-poor augite. This course of crystallization eventually joins the other course already pictured.

According to Tsuboi (1932), the pyroxenic components of magmas lying in the upper part of Fig. 2 separate Ca-rich clinopyroxene first, while those in the lower part of the same figure separate orthopyroxene first. The boundary between the two fields is the "two-pyroxene boundary."

The compositions of groundmass pyroxenes in equilibrium with phenocrysts of Ca-rich clinopyroxene alone should lie above this boundary line, while those in equilibrium with phenocrysts of orthopyroxene alone below this line. The former is represented by the pyroxenes Nos. 6 and 7, and the latter by Nos. 9 and 18. Therefore, in Fig. 2, the two-pyroxene boundary should be located below the points Nos. 6 and 7 and above the points Nos. 9 and 18. These are groundmass pyroxenes of basalts.

Again, the compositions of groundmass pyroxenes in equilibrium with phenocrysts of both Ca-rich clinopyroxene and orthopyroxene should lie on the two-pyroxene boundary. Such pyroxenes are Nos. 8, 12, and 13. Nos. 12 and 13 occur in rocks without pyroxene phenocrysts, but that they are in equilibrium with Ca-rich clinopyroxene and orthopyroxene phenocrysts is certain from the mineral assemblage of the associated lavas. They are pyroxenes of medium andesites and their compositions lie well below the boundary line already located. Most of the groundmass

pyroxenes of salic andesites in equilibrium with phenocrysts of both Ca-rich clinopyroxene and orthopyroxene have compositions closer to the Mg^{2+}—Fe^{2+} base of Fig. 2.

Thus the location of the two-pyroxene boundary moves toward the base of the figure as the proportion of the salic components of the magmas increases. If a tetrahedron is constructed with the *Wo-En-Fs* triangle as its base and with the salic components as its apex, the two-pyroxene boundary surface would rise from the base and gradually ap-

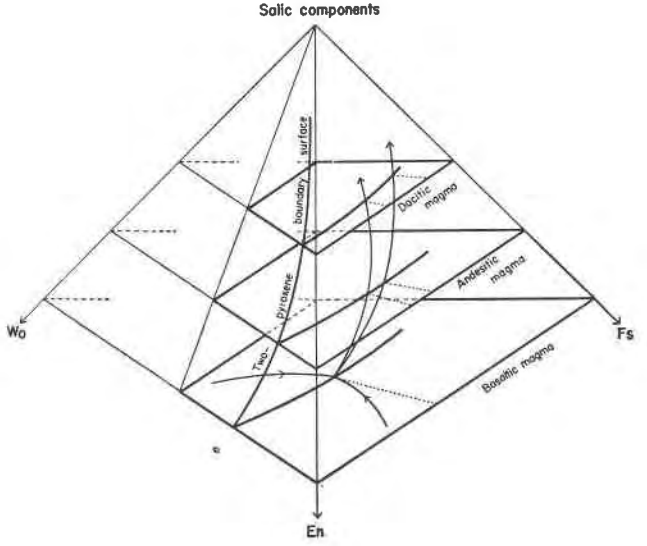

FIG. 7. Two-pyroxene boundary surface in a tetrahedron with *Wo-En-Fs* as its base and salic components as its apex. Three sections cut parallel to the base with different proportions of salic components are shown. The arrow heads indicate courses of crystallization of Japanese magmas.

proach the salic components-*En-Fs* face of the tetrahedron as shown in Fig. 7. The magmas would change their compositions along the curved courses of the figure, the difference of the courses depending on the original compositions and the degree of fractionation. In the triangular diagram Fig. 2, only the projections of various points lying on this surface are shown.

REFERENCES

AHRENS, L. H. (1952), The use of ionization potentials. Part 1. Ionic radii of the elements: *Geoch. Cosm. Acta*, **2**, 155–169.

ASKLUND, B. (1925), Petrological studies in the neighbourhood of Stavsjö at Kolmården. Granites and associated basic rocks of the Stavsjö area. *Sver. Geol. Undersök., ser. C, Årsbok*, **17**, 1–121.

ATLAS, L. (1952), The polymorphism of $MgSiO_3$ and solid-state equilibria in the system $MgSiO_3$—$CaMgSi_2O_6$: *J. Geol.*, **60,** 125–147.

BARTH, T. F. W. (1931*a*), Crystallization of pyroxenes from basalts: *Am. Mineral.*, **16,** 195–208.

BARTH, T. F. W. (1931*b*), Pyroxen von Hiva Oa, Marquesas-Inseln und die Formel titanhaltiger Augit: *Neues Jahrb. Min., Abt. A*, **64,** 217–224.

BARTH, T. F. W. (1951), Sub-solidus diagram of pyroxenes from common mafic magmas: *Norsk Geol. Tids.*, **29,** 218–221.

BENSON, W. N. (1944), The basic igneous rocks of Eastern Otago and their tectonic environment: *Tr. Roy. Soc. New Zealand*, **74,** 71–123.

BERMAN, H. (1937), Constitution and classification of natural silicates: *Am. Mineral.*, **22,** 333–415.

BOWEN, N. L. (1914), The ternary system: diopside—forsterite—silica: *Am. J. Sci.*, **38,** 207–264.

BOWEN, N. L. (1933), Crystals of iron-rich pyroxene from a slag: *J. Wash. Acad. Sci.*, **23,** 83–87.

BOWEN, N. L. (1935), "Ferrosilite" as a natural mineral: *Am. J. Sci.*, **30,** 481–494.

BOWEN, N. L., AND SCHAIRER, J. F. (1935), The system, MgO—FeO—SiO_2: *Am. J. Sci.*, **29,** 151–217.

BOWEN, N. L., SCHAIRER, J. F., AND POSNJAK, E. (1933), The system, CaO—FeO—SiO_2: *Am. J. Sci.*, **26,** 193–284.

DANA, J. D. (1900), System of mineralogy, 6th ed.: 352.

DIXON, B. E., AND KENNEDY, W. Q. (1933), Optically uniaxial titanaugite from Aberdeenshire: *Zeit. Krist., A*, **86,** 112–120.

EDWARDS, A. B. (1942), Differentiation of the dolerites of Tasmania: *J. Geol.*, **50,** 451–480; 579–610.

FAUST, G. T. (1936), The fusion relations of iron-orthoclase, with a discussion of the evidence for the existence of an iron-orthoclase molecule in feldspars: *Am. Mineral.*, **21,** 735–763.

HALLIMOND, A. F. (1914), Optically uniaxial augite from Mull: *Mineral. Mag.*, **17,** 97–99.

HESS, H. H. (1941), Pyroxenes of common mafic magmas: *Am. Mineral.*, **26,** 515–555; 573–579.

HESS, H. H. (1949), Chemical composition and optical properties of common clinopyroxenes: *Am. Mineral.*, **34,** 621–666.

HESS, H. H. (1952), Orthopyroxenes of the Bushveld type, ion substitutions and changes in unit cell dimensions: *Am. J. Sci., Bowen vol.*, 173–187.

KUNO, H. (1940), Pigeonite in the groundmass of some andesite from Hakone Volcano: *J. Geol. Soc. Japan*, **47,** 347–351.

KUNO, H. (1947), Occurrence of porphyritic pigeonite in "weiselbergite" from Weiselberg, Germany: *Proc. Japan Acad.*, **23,** 111–113.

KUNO, H. (1950), Petrology of Hakone Volcano and adjacent areas, Japan: *Bull. Geol. Soc. Am.*, **61,** 957–1020.

KUNO, H. (1952), Explanatory text of the geological map of Atami (in Japanese): *Geol. Surv. Japan*, sheet 123, 1–141.

KUNO, H. (1953), Formation of calderas and magmatic evolution: *Tr. Am. Geoph. Union*, **34,** 267–280.

KUNO, H., AND HESS, H. H. (1953), Unit cell dimensions of clinoenstatite and pigeonite in relation to other common clinopyroxenes: *Am. J. Sci.*, **251,** 741–752.

KUNO, H., AND INOUE, T. (1949), On porphyritic pigeonite in andesite from Ōkubo-yama, Minami-Aizu, Hukusima Prefecture: *Proc. Japan Acad.*, **25,** 128–132.

KUNO, H., AND NAGASHIMA, K. (1952), Chemical compositions of hypersthene and pigeonite in equilibrium in magma: *Am. Mineral.*, **37,** 1000–1006.

KUNO, H., AND SAWATARI, M. (1934), On the augites from Wadaki, Izu, and from Yoneyama, Etigo, Japan: *Jap. J. Geol. Geogr.*, **11,** 327–343.

MACDONALD, G. A. (1944), Pyroxenes in Hawaiian lavas: *Am. J. Sci.*, **242,** 626–629.

MINAKAMI, T. (1951*a*), Report on the volcanic activities in Japan during 1948–1950: *Intern. Ass. Vulc., Brussel, August* **1951,** 1–18.

MINAKAMI, T. (1951*b*), On the temperature and viscosity of the fresh lava extruded in the 1951 Oo-sima eruption: *Bull. Earthq. Res. Inst.*, **29,** 487–498.

MUIR, I. D. (1951), The clinopyroxenes of the Skaergaard intrusion, eastern Greenland: *Mineral. Mag.*, **29,** 690–714.

POLDERVAART, A., AND HESS, H. H. (1951), Pyroxenes in the crystallization of basaltic magma: *J. Geol.*, **59,** 472–489.

ROSENQVIST, I. TH. (1951), Investigations in the crystal chemistry of silicates. III. The relation haematite—microcline: *Norsk Geol. Tids.*, **29,** 65–76.

TSUBOI, S. (1932), On the course of crystallization of pyroxenes from rock-magmas: *Jap. J. Geol. Geogr.*, **10,** 67–82.

WAGER, L. R., AND DEER, W. A. (1939), Geological investigations in East Greenland. Pt. III. The petrology of the Skaergaard intrusion, Kangerdlugsuaq, East Greenland: *Medd. om Gronland*, **105,** no. 4, 1–352.

WAGER, L. R., AND MITCHELL, R. L. (1951), The distribution of trace elements during strong fractionation of basic magma—a further study of the Skaergaard intrusion, East Greenland: *Geoch. Cosm. Acta*, **1,** 131–208.

YODER, H. S. (1950), The jadeite problem, part I: *Am. J. Sci.*, **248,** 225–248.

Manuscript received Jan. 12, 1954